Surface Photochemistry of Bromoform on Ice: Cross Section and Competing Reaction Pathways

Mihail L. Grecea,*,† Ellen H. G. Backus,† Aart W. Kleyn,†,‡ and Mischa Bonn†,§

Leiden Institute of Chemistry, University of Leiden, Einsteinweg 55, P. O. Box 9502, 2300 RA Leiden, The Netherlands, FOM Institute for Plasma Physics Rijnhuizen, Euratom-FOM Association, P. O. Box 1207, 3430 BE Nieuwegein, The Netherlands, and FOM Institute for Atomic and Molecular Physics AMOLF, Kruislaan 407, 1098 SJ Amsterdam, The Netherlands

Received: May 17, 2005; In Final Form: July 14, 2005

The 266 nm photodissociation of bromoform adsorbed on an amorphous solid water (ASW) layer has been investigated for the first time under well-defined ultrahigh vacuum conditions. Time-of-flight (TOF) measurements indicate direct release of gas-phase Br, $CHBr_2$, Br_2, and CHBr species, with potential implications for stratospheric chemistry. Furthermore, new, ice-surface-mediated C−C ($C_2H_2Br_2$) and C−O (CHBrO, CO) species are revealed in postirradiation temperature programmed desorption (TPD) and reflection absorption infrared (RAIR) spectra. A cross section of $\sim 5 \times 10^{-20}$ cm^2 is determined for bromoform photodissociation at 266 nm based on the integrated area of both the TOF spectra of Br and Br_2 and the postirradiation TPD curves of $CHBr_3$. The involvement of the free, non-hydrogen-bonded water groups at the ASW surface in the formation of the photoproducts is evident from the RAIRS results.

1. Introduction

The role of chlorine- and bromine-containing compounds in stratospheric ozone depletion is well-known.[1−5] Heterogeneous reactions between stable halogen compounds on polar stratospheric cloud (PSC) particles are known to be key sources of molecules with increased photochemical activity.[1,3] The so-called type II PSC consists mostly of water ice,[6,7] and a typical reaction occurring on the surface of such particles is

$$HCl(ads) + ClONO_2(ads) \rightarrow Cl_2(g) + HNO_3(ads)$$

The subsequent ultraviolet (UV) light-induced decomposition of the gas-phase molecular chlorine leads to atomic Cl, which is highly active in ozone depletion.

In the stratosphere, bromine depletes ozone via a reaction mechanism similar to the ClO_x cycle:

$$\begin{aligned} Br + O_3 &\rightarrow BrO + O_2 \\ BrO + O &\rightarrow Br + O_2 \\ \hline O_3 + O &\rightarrow 2O_2 \end{aligned}$$

Although the concentration of bromine in the stratosphere is significantly lower than that of chlorine, bromine has been recognized to be far more destructive to stratospheric ozone than chlorine on a per-atom basis.[8] Recent reports have estimated the ozone destruction potential of bromine to be up to 2 orders of magnitude higher than that of chlorine.[9,10] Moreover, the synergism of bromine and chlorine cycles[4] can significantly enhance ozone depletion by releasing free bromine and chlorine atoms via the reaction

$$BrO + ClO \rightarrow Br + Cl + O_2$$

Photochemical studies on atmospherically relevant halocarbon compounds have revealed the UV-induced fragmentation of methyl bromide (CH_3Br) on Pt(111)[11] and on Br-precovered Ni(111).[12] The photochemistry of CD_3Cl trapped and caged inside thin (≤20 monolayers) amorphous solid water (ASW) layers on Ru(001) has been studied recently, with reports of new C−C and C−O bond containing species.[13]

Bromoform ($CHBr_3$) is one of the halocarbon compounds that supply active bromine to the atmosphere. It is mainly produced by ice algae as a byproduct of the photosynthetic process[14] and by emissions from oceanic microalgae.[15] The importance of bromoform as a dominant source of stratospheric bromine has been the subject of recent debate,[9] but its presence in the stratosphere is undebated,[16,17] and its contribution to stratospheric inorganic bromine has been reported to be higher than that of conventional sources, such as halons and methyl bromide.[18] Photodissociation studies on gas-phase bromoform have been reported only recently for various irradiation wavelengths.[19−23] Regardless of the wavelength in the range of 193−267 nm, prompt C−Br bond cleavage is the dominant single-photon dissociation channel. Furthermore, Br_2 elimination has been recently reported as an additional primary channel between 234 and 267 nm.[20,22]

Bromoform may adsorb on the surface of ice particles in the polar stratospheric clouds. An unexpectedly high mobility of bromoform molecules adsorbed on ice surfaces, compared with their chlorine counterparts, has been recently reported.[24] The precise adsorption structure may also influence the photochemistry of bromoform (i) by inhibiting the photodissociation owing to energy transfer to ice and/or desorption, (ii) by affecting the

* Corresponding author. E-mail: m.grecea@chem.leidenuniv.nl. Phone: +31-71-5274452. Fax: +31-71-5274451.
† University of Leiden.
‡ FOM Institute for Plasma Physics Rijnhuizen.
§ FOM Institute for Atomic and Molecular Physics AMOLF.

10.1021/jp052586n CCC: $30.25
Published on Web 08/27/2005

relative yields of the photoproducts, and (iii) by subsequent interaction of the photoproducts with the ice surface, following the primary photochemical event. The possible influence of the interaction with ice on the bromoform photochemistry has not been investigated to date, to the best of our knowledge, despite the significant contribution of bromoform to the halogen atmospheric chemistry.

Here, we present the first photodissociation study of bromoform adsorbed on ice surfaces in ultrahigh vacuum (UHV) using pulsed laser irradiation. We present results from time-of-flight (TOF), postirradiation reflection absorption infrared spectroscopy (RAIRS), and temperature programmed desorption (TPD) experiments. Our results demonstrate rich chemistry upon 266 nm irradiation of bromoform on ASW. Two distinct chemical pathways are revealed: first, direct photoproducts are evident from the TOF spectra, producing Br, $CHBr_2$, Br_2, and CHBr, in agreement with the single-photon dissociation diagram of gas-phase $CHBr_3$.[23] Second, new, ice-mediated C−O and C−C species are visible in postirradiation RAIRS and TPD results. The active involvement of the ice matrix in the formation of C−O species is evidenced by the disappearance of the peak characteristic to the "dangling" O−H (O−D) bonds in the postirradiation RAIR spectrum of the bromoform−water system.

2. Experimental Section

The experiments were carried out in a UHV chamber[25,26] with a base pressure of 3×10^{-11} mbar. A triply differentially pumped, compact molecular beam line was used for dosing water onto an inert, single-crystal platinum substrate. This Pt(533) substrate was mounted on a liquid nitrogen cooled, temperature-controlled sample holder. Details of the experimental setup and substrate cleaning procedures can be found elsewhere.[27]

Compact, nonporous ASW layers were prepared by depositing water from the molecular beam under normal incidence at a substrate temperature of 100 K (at a deposition rate of ∼5 monolayers (ML) min^{-1}). Uniform layers can be deposited, as the diameter of the molecular beam at the crystal position exceeds that of the crystal. Unless otherwise mentioned, the thickness of the ASW layers in the experiments amounted to 65 ML. One water monolayer is defined as the dose of water necessary to form an ice-like bilayer on the Pt(533) substrate, as defined in refs 27 and 28, so that the layer is effectively 130 water layers thick. The results presented here were found to be insensitive to the ASW layer thickness (between 40 and 80 ML), indicating that the metal substrate plays no significant role in the photochemical processes. Experiments on thinner ASW layers reveal that the Pt substrate plays an important role in the surface chemistry for layers thinner than ∼10 ML, enabling new reaction pathways. This, however, is outside the scope of this paper.

Bromoform molecules were adsorbed onto the ASW layer at 100 K by background dosing of $CHBr_3$ (>99%, Aldrich), typically at a pressure of 1×10^{-7} mbar. The exposure was controlled by varying the dosing time. A dose of 10 L (we define 1 langmuir (L) ≡ 1×10^{-6} mbar s) $CHBr_3$ results in 1 ML (monolayer) on the ice surface. (In our previous study,[24] it was erroneously mentioned that 1 ML coverage is reached at 5 L. This does not affect the conclusions presented here, or in ref 24, however.) In this study, 1 ML of $CHBr_3$ is defined as the coverage above which the multilayer desorption peak starts appearing in the TPD spectrum. The reported pressures are not corrected for ion-gauge sensitivity.

Photochemical processes were initiated using irradiation at 266 nm, obtained by tripling the output of an amplified Ti:sapphire laser (Quantronix GmbH). The laser provides pulses of 130 fs duration at 266 nm of about 90 μJ/pulse at a repetition rate of 1 kHz. The substrate was homogeneously irradiated at a 35° angle with respect to the surface normal, using a spot size exceeding the substrate diameter. Using the resulting low laser fluence (∼1 $J \cdot m^{-2}$), the contribution from multiphoton processes was absent. The ice is transparent to this wavelength,[29] and most of the incident energy is absorbed by the Pt substrate. Absorption of 65% of the laser light by the substrate results in a transient substrate heating less than 10 K during the laser pulse duration, and therefore any thermal reactivity of the adsorbed molecules can be ruled out. The photochemistry occurs through direct absorption of single 266 nm photons (photon energy 4.5 eV) by the adsorbed bromoform. Moreover, no change in the RAIR spectrum of D_2O is observed after irradiation (see Figure 4). Photodesorbed fragments were detected as a function of their flight time by a differentially pumped quadrupole mass spectrometer (QMS, Balzers QS 422) placed in a collinear geometry with the sample surface normal, amplified with a fast amplifier, and counted with a multichannel scaler after a 70 mm flight path. The same mass spectrometer was used to record postirradiation TPD spectra. Masses 18 (H_2O^+), 108 ($CHBrO^+$), 171 ($CHBr_2^+$), 187 ($C_2H_2Br_2^+$), and 252 ($CHBr_3^+$) were simultaneously monitored. TPD spectra were typically recorded at a heating rate of 0.5 K s^{-1}.

The IR absorption (RAIR) spectra were recorded at 4 cm^{-1} resolution under grazing incidence with a commercial Fourier transform infrared (FTIR) spectrometer (Bio-Rad FTS 175). For the RAIRS measurements, D_2O was used instead of H_2O, to prevent the C−H stretching vibration of $CHBr_3$ at 3017 cm^{-1} from being obscured by the O−H stretching mode region of H_2O (3000−3700 cm^{-1}).

3. Results and Discussion

Time-of-flight (TOF) spectra of Br^+ (*m*/*z* 79), $CHBr_2^+$ (*m*/*z* 171), Br_2^+ (*m*/*z* 158), and $CHBr^+$ (*m*/*z* 92), collected during the 266 nm irradiation of 10 L $CHBr_3$ adsorbed on 65 ML of ASW, are shown in Figure 1 (top panel). The TOF spectra are averages of 60 000 laser pulses, and can be well described by Maxwell−Boltzmann distributions,[30] with the corresponding translational temperatures indicated in the graph. The observed photoproducts are in good agreement with the energetically allowed single-photon dissociation channels (Br + $CHBr_2$ and Br_2 + CHBr).[23] The translational temperatures are much higher than the temperature of the underlying ASW (100 K), indicating that the photoproducts are not thermalized[31,32] with the ASW substrate. No $CHBr_3$ (*m*/*z* 252) desorption could be detected within the detection limits of our setup. Moreover, it is highly unlikely that the detected Br originates from cracking of $CHBr_3$ in the QMS ionizer, as this would imply unphysically large translational temperatures for $CHBr_3$. The translational temperatures in Figure 1 (top panel) reflect the particular translational gain of every photoproduct as a result of the photon energy, as well as the precise reaction pathway and further collision events prior to ejection. It is evident, however, that the higher translational energy of the first channel fragments (Br + $CHBr_2$) is consistent with the large amount of excess energy associated with that channel of $CHBr_3$ dissociation.[23] The dependence of the photochemical yield on the photon flux is depicted in Figure 1 (bottom panel) for the indicated masses. The yield was obtained from the integrated area of the TOF spectra successively measured on the same $CHBr_3$ sample. The cross sections (σ', σ'') extracted from the slope of the decay curves in Figure 1 (bottom panel) are discussed below. Note that bromine atom

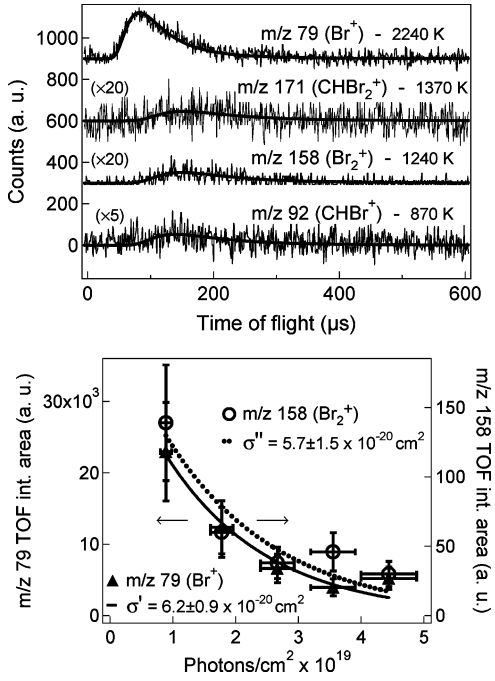

Figure 1. Top panel: TOF spectra of Br^+ (*m*/*z* 79), $CHBr_2^+$ (*m*/*z* 171), Br_2^+ (*m*/*z* 158), and $CHBr^+$ (*m*/*z* 92), following irradiation of 10 L $CHBr_3$ adsorbed on 65 ML of ASW by laser pulses at 266 nm, at $t = 0$. The distribution of flight times of the different fragments from the surface to the mass spectrometer (7 cm from the surface) is characterized by translational temperatures indicated in the graph. These temperatures are obtained from a fit to Maxwell−Boltzmann distributions, shown as solid black lines. Bottom panel: Dependence of the *m*/*z* 79 (Br^+) and *m*/*z* 158 (Br_2^+) yields on the number of photons (solid symbols), determined from the integrated area of the corresponding TOF spectra measured on the same $CHBr_3$ sample. (The TOF spectra of Br^+ and Br_2^+ desorbed upon the irradiation by 8.9×10^{18} cm^{-2} photons are shown in the top panel.) Horizontal error bars indicate the fluence integration limits for each point. The indicated cross sections (σ', σ'') are given by the slope of a single exponential fit trace.

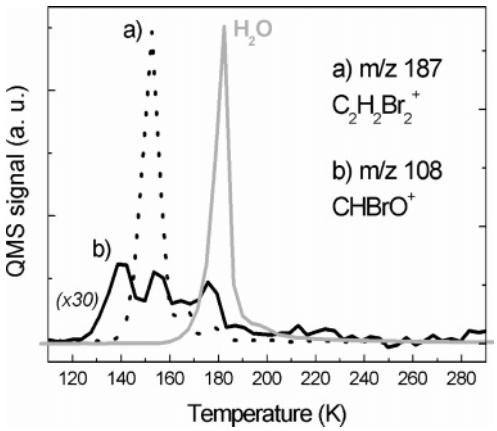

Figure 2. Postirradiation TPD spectra (heating rate 0.5 K s^{-1}) at indicated masses, following irradiation of 10 L $CHBr_3$ dosed on 65 ML of ASW by 8.9×10^{18} cm^{-2}, 266 nm photons. The gray curve depicts the scaled TPD spectrum of multilayer ASW (*m*/*z* 18).

abstraction from neighbor bromoform to form diatomic (Br_2) species cannot be excluded as a source for molecular Br_2.

More complex photoproducts containing, for example, C−C and C−O bonds were not observed to desorb upon irradiation in TOF measurements, but are clearly present in postirradiation TPD spectra as shown in Figure 2 (dotted curve a, *m*/*z* 187 ($C_2H_2Br_2^+$), and continuous curve b, *m*/*z* 108 ($CHBrO^+$)). TPDs were recorded for an initial exposure of 10 L $CHBr_3$ on a 65

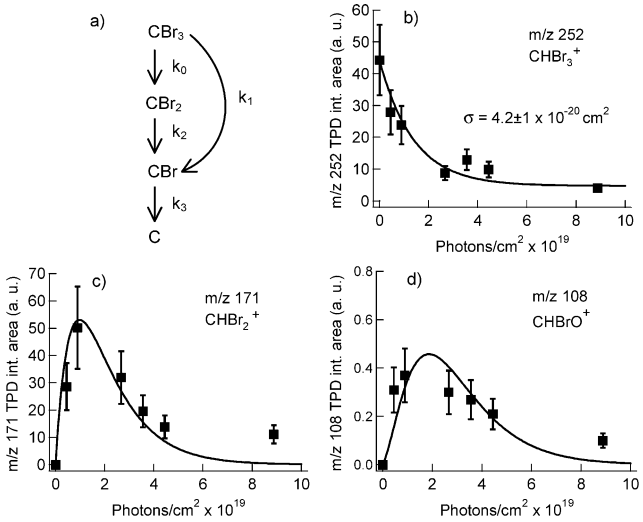

Figure 3. (a) Schematic model proposed for UV induced reaction pathways of $CHBr_3$ adsorbed on ASW. The k_i ($i = 0-3$) parameters correspond to the cross section of the indicated processes. (b−d) Photochemical yield for the $CHBr_3$ depletion (b) and formation of the indicated photoproducts (c, d), following 266 nm irradiation of 10 L $CHBr_3$ adsorbed on 65 ML of ASW (solid symbols). The yield was determined from the integrated area of the corresponding postirradiation TPD curves (not shown). The fit curves (b−d) were obtained on the basis of the model shown in graph a. The cross section of the $CHBr_3$ depletion (σ) was extracted from the slope of a single exponential fitting curve (b).

ML thick ASW layer, following irradiation by 8.9×10^{18} cm^{-2} photons. Note that, in these TPD measurements, reaction products of both thermal and nonthermal components of the photochemistry are observed. These ice-surface-mediated photoproducts (not observed in the absence of radiation) are formed through two distinct reaction channels: first, the interaction of $CHBr_2$/CHBr with water molecules of the ice matrix results in the formation of C−O bonds (CHBrO). These photoproducts are consistent with previous calculations that indicate CHBrO as intermediate products of the water-catalyzed photodissociation of $CHBr_3$ in aqueous solution.[33] Second, it is clear that dimerization of CHBr photofragments, leading to the formation of $C_2H_2Br_2$, is observed.

It is obvious that the first reaction step in the formation of all the aforementioned compounds is the photoinduced C−Br bond rupture. To determine the cross sections of Br abstraction from $CHBr_3$ and subsequent photoproducts (e.g., $CHBr_2$), the yield of the various photoproducts was studied using the TPD integrated area as a function of photon flux, as shown in Figure 3b−d (solid symbols). The $CHBr_2$ signal is a measure of the single-bromine abstraction reaction, and the CHBrO, of double-Br abstraction. A scheme employed to model the photoreaction pathways is given in Figure 3a (where k_i ($i = 0-3$) indicates the cross section of the mentioned processes). The results are shown as lines in Figure 3b−d. The ratio between the cross section for single and simultaneous double Br abstraction (k_0: k_1) is set to be 5:1, as in previous reports of the branching ratio of the gas-phase $CHBr_3$ dissociation at this wavelength.[20] (Due to the unknown QMS sensitivity difference between Br and Br_2, we have not been able to determine this ratio from our experiments.) The results of Figure 3c,d can be reproduced with $k_2 \sim 2\sigma$ and $k_3 \sim 1.4\sigma$ (with $\sigma = k_0 + k_1$). Note that k_2 and k_3 are compound, effective reaction rates that also include the disappearance of CBr and CBr_2 species due to dimerization and other thermal reactions, in addition to photochemical Br abstraction. The cross section of $CHBr_3$ depletion ($\sigma = k_0 +$

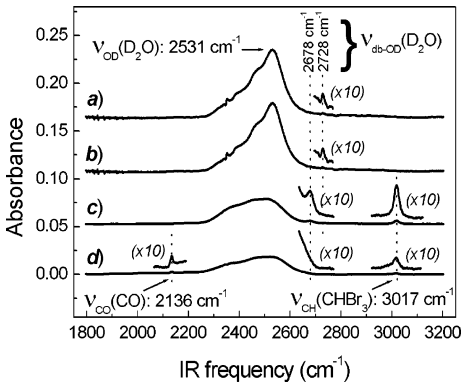

Figure 4. (a) RAIR spectrum of 22 ML of D_2O adsorbed (at 100 K) on Pt(533), shown in the frequency range of 1800−3200 cm^{-1}. (b) Postirradiation RAIR spectrum of the D_2O sample following irradiation by 8.9×10^{18} photons cm^{-2} at a wavelength of 266 nm. (c) RAIR spectrum of 10 L $CHBr_3$ adsorbed on top of 22 ML of D_2O and 90 L $CHBr_3$ simultaneously dosed (at 100 K) on Pt(533). (d) Postirradiation RAIR spectrum of the $D_2O-CHBr_3$ sample following irradiation by 8.9×10^{18} photons cm^{-2} at a wavelength of 266 nm. All RAIR spectra were measured at 100 K. The weak features in the spectra a and b at ~2355 cm^{-1} is due to the incomplete cancellation of gas-phase CO_2 present in the optical path in that set of experiments.

k_1) can be determined not only from the TOF measurements (see above), but also from the postirradiation TPD results. The plot of the integrated area of the postirradiation TPD curves of $CHBr_3$ as a function of photon flux (Figure 3b) reveals a cross section of $(4.2 \pm 1) \times 10^{-20}$ cm^2 for $CHBr_3$ depletion, which is in reasonable agreement with the values obtained from the TOF results for the Br [$(6.2 \pm 0.9) \times 10^{-20}$ cm^2] and Br_2 [$(5.7 \pm 1.5) \times 10^{-20}$ cm^2] formation, but lower than the cross section of gas-phase $CHBr_3$ at 248 nm (1.9×10^{-18} cm^2).[21] In addition, the cross section found for $CHBr_3$ depletion is slightly lower than that of the CH_3Br photofragmentation on Br/Ni(111) at 193 nm [$(8.4 \pm 0.6) \times 10^{-20}$ cm^2][12] and lies between the values obtained in the case of CD_3Cl photoinduced dissociation at 193 nm [$(1-6) \times 10^{-19}$ cm^2] and at 248 nm [$(1-3) \times 10^{-20}$ cm^2].[13] Several effects can be included into the cross section in addition to direct $CHBr_3$ photofragmentation. Caging effects of the $CHBr_3$ molecules at higher coverages, similar to CH_3Br on Pt(111),[11] could occur, decreasing the apparent cross section. Recombination of trapped photofragments during TPD will also reduce the cross section. In contrast, the photofragments produced could be sufficiently energetic to eject adjacent molecules, thus increasing the depletion cross section. Although desorption electron attachment (DEA) cannot be completely ruled out as a contribution to $CHBr_3$ depletion, this excitation mechanism is active a limited distance from the substrate surface.[12,34] Our data suggest that this contribution is negligibly small for ASW thickness between 40 and 80 ML, as the production rate of the photofragments is constant over this ASW thickness domain.

In this model we proposed that bromoform can be completely stripped of its bromine atoms, which has also been reported for the 240 nm photolysis of $CHBr_3$ in aqueous solution.[33] Indeed, with RAIRS we observed the formation of a small amount of CO molecules as well. Most likely, among CBr species, CHBrO dissociation represents the origin of this CO, as the Br−CO binding energy is only 0.3 kcal/mol.[35] Figure 4 depicts RAIR spectra (at 100 K) in the frequency range of 1800−3200 cm^{-1} of (a) pure D_2O adsorbed on Pt(533), (b) after irradiation of the D_2O sample, (c) $CHBr_3$ on top of the $CHBr_3$:D_2O coadsorption system, and (d) after irradiation of the latter. Figure 4a is consistent with previous IR spectra of ASW (D_2O) adsorbed on Pt(111) and W(100) substrates:[36,37] a broad band of the O−D stretching vibration, centered at 2531 cm^{-1}, with a small, sharp peak at 2728 cm^{-1}, corresponding to the unsaturated surface OD bonds. The spectrum of 10 L $CHBr_3$ adsorbed on top of 22 ML of D_2O and 90 L $CHBr_3$ simultaneously dosed (at 100 K) on Pt(533) is depicted in Figure 4c. It is obvious that, in the case of the $CHBr_3$ occluded within the ASW matrix, the TOF signal of Br and Br_2 would be significantly decreased and the cross section of the photoinduced events would change due to the caging effect following the coadsorption procedure. However, the simultaneous adsorption ensures a larger exposure of the D_2O ice matrix to the $CHBr_3$ molecules and, consequently, sufficient optical density to record RAIR spectra of $CHBr_3$ and its (photo)products. Similar to earlier studies on codeposited $CHBr_3-D_2O$,[38] a shift of 50 cm^{-1} to lower wavenumbers can be observed for the "dangling" OD vibration of amorphous D_2O (2678 cm^{-1}). This shift is an indication for the halomethane interaction through lone pair donation from a halogen atom to a deuterium atom of the water molecule.[38] (Co)adsorbed onto ASW, the C−H stretching vibration of $CHBr_3$, at 3017 cm^{-1} (Figure 4c), is slightly shifted from the argon matrix (3063 cm^{-1})[39,40] and gas-phase (3048 cm^{-1} [41]−3050 cm^{-1} [40,42]) peak positions. Postirradiation RAIR spectra (Figure 4d) reveal that the intensity of the CH peak of $CHBr_3$ weakens, after irradiation by 8.9×10^{18} photons cm^{-2}. At the same time, a new peak appears at 2136 cm^{-1}, in very good agreement with the previously reported IR vibration of CO entrapped in an ASW matrix.[43] From the integrated area of the RAIRS peaks we conclude that roughly ~1% of $CHBr_3$ is converted to CO for this photon dose, i.e., too little to be observed in the postirradiation TPD spectrum of 10 L $CHBr_3$ on pure ASW as shown in Figures 2 and 3.

The most remarkable feature in the RAIR spectra is the essentially complete disappearance of the resonance associated with the unsaturated, "dangling" surface OD bonds upon irradiation of the $CHBr_3$ adsorbed on the $CHBr_3$:D_2O system (Figure 4d). As the mentioned peak is visible in the postirradiation RAIR spectrum of pure D_2O (Figure 4b), these observations strongly suggest that the surface O−D bonds are highly active in the surface photochemistry of $CHBr_3$.

The observations in the present work may have important implications for atmospheric chemistry, particularly for ozone depletion. As direct Br, $CHBr_2$, Br_2, and CHBr photoproducts arise from the photodissociation of ice supported $CHBr_3$, this system may constitute a significant source for the release of gas-phase bromine species in the stratosphere. The photochemistry of bromine-containing species may also account for their anomalous reactivity[8−10] in heterogeneous processes related to ozone depletion. Additional Br is liberated by photoexcitation of $CHBr_2$, CHBr, Br_2, and $C_2H_2Br_2$, as indicated both by the model described above (for $CHBr_2$, CHBr) and in previous reports.[44,45]

The photochemistry of the bromine compounds also induces irreversible chemical transformations of the ice surface, principally involving the unsaturated hydroxyl groups. This might have implications for some heterogeneous reactions leading to ozone depletion, reported to depend on the nature of the stratospheric particles' surface.[7]

4. Conclusions

Photodissociation studies of $CHBr_3$ on amorphous solid water at 266 nm irradiation have been reported for the first time. Various fragmentation pathways, as well as new, ice-mediated C−C and C−O bond containing species have been revealed by

TOF, and postirradiation TPD and RAIRS results. Direct Br, $CHBr_2$, Br_2, and CHBr photoproducts are released as a result of direct molecular absorption at 266 nm irradiation. In addition, surface-induced photoproduct reactions, e.g., CHBr dimerization, take place. CHBrO and CO formation, presumably due to the active involvement of the ice matrix water molecules, is also observed. The cross section for ASW supported $CHBr_3$ photodissociation at 266 nm irradiation is observed to be $(5 \pm 2) \times 10^{-20}$ cm^2. These results illustrate a rich photochemistry of bromoform on the ice surface, which may have significant implications for current atmospheric chemical models, particularly in accurately estimating the abundance of (bromine) species released from bromoform following its UV dissociation in the atmosphere.

Acknowledgment. The authors would like to thank T. Pradeep for his contribution to the start of this work, and O. Berg for expert help with RAIRS analysis. This work is part of the research program of the Stichting voor Fundamenteel Onderzoek der Materie (FOM), which is financially supported by the Nederlandse organisatie voor Wetenschappelijk Onderzoek (NWO).

References and Notes

(1) Bedjanian, Y.; Poulet, G. *Chem. Rev.* **2003**, *103*, 4639.
(2) Geller, M. A.; Yudin, V.; Douglass, A. R.; Waters, J. W.; Elson, L. S.; Roche, A. E.; Russell, J. M. *Geophys. Res. Lett.* **1995**, *22*, 2937.
(3) Klan, P.; Holoubek, I. *Chemosphere* **2002**, *46*, 1201.
(4) Salawitch, R. J.; Weisenstein, D. K.; Kovalenko, L. J.; Sioris, C. E.; Wennberg, P. O.; Chance, K.; Ko, M. K. W.; McLinden, C. A. *Geophys. Res. Lett.* **2005**, *32*, L05811.
(5) Siskind, D. E.; Froidevaux, L.; Russell, J. M.; Lean, J. *Geophys. Res. Lett.* **1998**, *25*, 3513.
(6) Schreiner, J.; Voigt, C.; Kohlmann, A.; Arnold, F.; Mauersberger, K.; Larsen, N. *Science* **1999**, *283*, 968.
(7) Wayne, R. P. *Chemistry of Atmospheres*, 3rd ed.; Oxford University Press: Oxford, 2000.
(8) WMO. *Scientific assessment of Ozone Depletion: 1994*; WMO: Geneva, Switzerland, 1995.
(9) Garcia, R. R.; Solomon, S. *J. Geophys. Res., [Atmos.]* **1994**, *99*, 12937.
(10) Solomon, S.; Mills, M.; Heidt, L. E.; Pollock, W. H.; Tuck, A. F. *J. Geophys. Res., [Atmos.]* **1992**, *97*, 825.
(11) French, C.; Harrison, I. *Surf. Sci.* **1997**, *387*, 11.
(12) Marsh, E. P.; Tabares, F. L.; Schneider, M. R.; Gilton, T. L.; Meier, W.; Cowin, J. P. *J. Chem. Phys.* **1990**, *92*, 2004.
(13) Lilach, Y.; Asscher, M. *J. Chem. Phys.* **2003**, *119*, 407.
(14) Cota, G. F.; Sturges, W. T. *Mar. Chem.* **1997**, *56*, 181.
(15) Carpenter, L. J.; Sturges, W. T.; Penkett, S. A.; Liss, P. S.; Alicke, B.; Hebestreit, K.; Platt, U. *J. Geophys. Res., [Atmos.]* **1999**, *104*, 1679.
(16) Sturges, W. T.; Oram, D. E.; Carpenter, L. J.; Penkett, S. A.; Engel, A. *Geophys. Res. Lett.* **2000**, *27*, 2081.
(17) Nielsen, J. E.; Douglass, A. R. *J. Geophys. Res., [Atmos.]* **2001**, *106*, 8089.
(18) Dvortsov, V. L.; Geller, M. A.; Solomon, S.; Schauffler, S. M.; Atlas, E. L.; Blake, D. R. *Geophys. Res. Lett.* **1999**, *26*, 1699.
(19) McGivern, W. S.; Sorkhabi, O.; Suits, A. G.; Derecskei-Kovacs, A.; North, S. W. *J. Phys. Chem. A* **2000**, *104*, 10085.
(20) Xu, D. D.; Francisco, J. S.; Huang, J.; Jackson, W. M. *J. Chem. Phys.* **2002**, *117*, 2578.
(21) Zou, P.; Shu, J. N.; Sears, T. J.; Hall, G. E.; North, S. W. *J. Phys. Chem. A* **2004**, *108*, 1482.
(22) Huang, H. Y.; Chuang, W. T.; Sharma, R. C.; Hsu, C. Y.; Lin, K. C.; Hu, C. H. *J. Chem. Phys.* **2004**, *121*, 5253.
(23) Lindner, J.; Ermisch, K.; Wilhelm, R. *Chem. Phys.* **1998**, *238*, 329.
(24) Grecea, M. L.; Backus, E. H. G.; Fraser, H. J.; Pradeep, T.; Kleyn, A. W.; Bonn, M. *Chem. Phys. Lett.* **2004**, *385*, 244.
(25) Riedmuller, B.; Giskes, F.; van Loon, D. G.; Lassing, P.; Kleyn, A. W. *Meas. Sci. Technol.* **2002**, *13*, 141.
(26) Jenniskens, H. G.; Bot, A.; Dorlandt, P. W. F.; vanEssenberg, W.; deHaas, E.; Kleyn, A. W. *Meas. Sci. Technol.* **1997**, *8*, 1313.
(27) Grecea, M. L.; Backus, E. H. G.; Riedmuller, B.; Eichler, A.; Kleyn, A. W.; Bonn, M. *J. Phys. Chem. B* **2004**, *108*, 12575.
(28) Smith, R. S.; Dohnalek, Z.; Kimmel, G. A.; Stevenson, K. P.; Kay, B. D. *Chem. Phys.* **2000**, *258*, 291.
(29) Chakarov, D.; Kasemo, B. *Phys. Rev. Lett.* **1998**, *81*, 5181.
(30) Hasselbrink, E. State-Resolved Probes of Molecular Desorption Dynamics Induced by Short-Lived Electronic Excitations. In *Laser Spectroscopy and Photo-chemistry on Metal Surfaces*; Dai, H.-L., Ho, W., Eds.; World Scientific: Singapore, 1995.
(31) Jenniskens, H. G.; Philippe, L.; Kadodwala, M.; Kleyn, A. W. *J. Phys. Chem. B* **1998**, *102*, 8736.
(32) Fieberg, J. E.; White, J. M. *Chem. Phys. Lett.* **1999**, *306*, 103.
(33) Kwok, W. M.; Zhao, C. Y.; Li, Y. L.; Guan, X. G.; Wang, D. G.; Phillips, D. L. *J. Am. Chem. Soc.* **2004**, *126*, 3119.
(34) Gilton, T. L.; Dehnbostel, C. P.; Cowin, J. P. *J. Chem. Phys.* **1989**, *91*, 1937.
(35) Dixon, D. A.; Peterson, K. A.; Francisco, J. S. *J. Phys. Chem. A* **2000**, *104*, 6227.
(36) Schaff, J. E.; Roberts, J. T. *J. Phys. Chem.* **1996**, *100*, 14151.
(37) Schaff, J. E.; Roberts, J. T. *Langmuir* **1998**, *14*, 1478.
(38) Holmes, N. S.; Sodeau, J. R. *J. Phys. Chem. A* **1999**, *103*, 4673.
(39) Lasson, E.; Nielsen, C. J. *Acta Chem. Scand.* **1997**, *51*, 1.
(40) Venkatraman, R.; Kwiatkowski, J. S.; Bakalarski, G.; Leszczynski, J. *Mol. Phys.* **2000**, *98*, 371.
(41) Kamboures, M. A.; Hansen, J. C.; Francisco, J. S. *Chem. Phys. Lett.* **2002**, *353*, 335.
(42) Rogers, E. E.; Abramowitz, S.; Jacox, M. E.; Milligan, D. E. *J. Chem. Phys.* **1970**, *52*, 2198.
(43) Collings, M. P.; Dever, J. W.; Fraser, H. J.; McCoustra, M. R. S.; Williams, D. A. *Astrophys. J.* **2003**, *583*, 1058.
(44) Wofsy, S. C.; McElroy, M. B.; Yung, Y. L. *Geophys. Res. Lett.* **1975**, *2*, 215.
(45) Lee, Y. R.; Chou, C. C.; Lee, Y. J.; Wang, L. D.; Lin, S. M. *J. Chem. Phys.* **2001**, *115*, 3195.